

# A Mechanism for the Oxygen and Iron Bimodal Radial Distribution Formation in the Disc of our Galaxy

I. A. Acharova,<sup>1\*</sup> J. R. D. Lépine,<sup>2</sup> Yu. N. Mishurov,<sup>1,3</sup> B.M.Shustov,<sup>4</sup> A.V.Tutukov,<sup>4</sup> and D.S. Wiebe<sup>4</sup>

<sup>1</sup> Department of Physics of Cosmos, Southern Federal University, 5 Zorge, Rostov-on-Don, 344090, Russia

<sup>2</sup> Instituto de Astronomia, Geofísica e Ciências Atmosféricas, Universidade de São Paulo, Cidade Universitária, São Paulo, SP, Brazil

<sup>3</sup> Special Astrophysical Observatory of Russian Academy of Sciences, N.Arkhyz, Karachaevo-Cherkessia, Russia

<sup>4</sup> Institute of Astronomy of the Russian Academy of Sciences, 48 Pyatnitskaya St., Moscow, 119017, Russia

Accepted 2009 xxxx. Received 2009 xxxx; in original form 2009 xxxx

## ABSTRACT

Recently it has been proposed that there are two types of SN Ia progenitors – short-lived and long-lived. On the basis of this idea, we develop a theory of a unified mechanism for the formation of the bimodal radial distribution of iron and oxygen in the Galactic disc. The underlying cause for the formation of the fine structure of the radial abundance pattern is the influence of spiral arms, specifically, the combined effect of the corotation resonance and turbulent diffusion. From our modelling we conclude that to explain the bimodal radial distributions simultaneously for oxygen and iron and to obtain approximately equal total iron output from different types of supernovae, the mean ejected iron mass per supernova event should be the same as quoted in literature if maximum mass of stars, that eject heavy elements, is  $50 M_{\odot}$ . For the upper mass limit of  $70 M_{\odot}$  the production of iron by a supernova II explosion should be increased by about 1.5 times.

**Key words:** Galaxy: abundances – Galaxy: structure.

## 1 INTRODUCTION

Galactic nucleosynthesis studies provide a very important information about the structure and evolution of the Milky Way Galaxy, since chemical abundances accumulate and retain signatures of milestones in its history. This is why this research area is often called the “cosmic archaeology”. Knowledge of heavy element enrichment in galaxies plays a crucial role in various scientific areas.

One of the most prominent features of the chemical composition both in the Milky Way and other galaxies is the metallicity gradient. For a long time, it was widely believed that the radial metallicity distribution in galactic discs is described simply by a linear function, with the more or less constant gradient value being typical for the most part of the disc (see e.g. Wielen et al. 1996).

Such an oversimplified belief was first broken by Shaver et al. (1983) and Twarog et al. (1997). They concluded that the abundance distribution in the disc of the Galaxy is not described by a linear function with a constant slope. In a series of papers, Andrievsky et al. (2002, hereafter A02), Luck et al. (2006, hereafter LKA06) and others, have shown that in the Milky Way, oxygen and iron demonstrate a bimodal distribution along the galactic radius. In the inner part, from about 4 to 6.6 kpc, the gradient is

quite steep (for iron it is of the order of  $-0.13 \text{ dex/kpc}$ ), whereas in the outer part, approximately from 6.6 to 10.6 kpc, the distribution is plateau-like (the gradient is about  $-0.03 \text{ dex/kpc}$ , which is about 4 times smaller in absolute value than in the inner part), the distributions being similar both for oxygen and iron.

This result has posed a very difficult problem that remained unsolved for several years. Indeed, at the epoch, when most researches believed that the abundance radial distribution is linear, they did not pay much attention to the fact that the gradients show up in observations of different elements. They also did not worry about that oxygen and iron have close radial distribution in the disc of the Galaxy. The reason perhaps was as follows. The radial distributions of both types of SNe, averaged over the azimuthal angle in the galactic plane, are approximately exponential with close radial scales. Hence, we may expect that the abundances, expressed in the logarithmic scale, will be approximately linearly distributed along the galactic radius with close gradient values. But the bimodal radial abundance pattern breaks this oversimplified representation.

In the present paper, we continue the research started by Mishurov et al. (2002) and Acharova et al. (2005). In the cited papers and others a theory of formation the bimodal abundance pattern under the influence of spiral arms was developed. The main cause for formation of the bimodal distribution is assumed to be the **corotation** resonance which is located close to the solar galactocentric distance (e.g. Lépine et al. 2001, and papers cited therein). In the previous papers we have only considered the enrichment of

\* E-mail: iaacharova@sfedu.ru (IAA); jacques@astro.iag.usp.br (JRDL); unmishurov@sfedu.ru (YuNM); bshustov@inasan.ru (BMS); atutukov@inasan.ru (AVT); dwiebe@inasan.ru (DSW)

the interstellar medium (ISM) by oxygen, because the main source of oxygen – SN II – are strongly concentrated in spiral arms. Their progenitors are massive stars with extremely short life-time, thus, SN II do not escape from spiral arms where they were born. Hence, oxygen is the most obvious indicator for the arm influence on nucleosynthesis (see details in the papers cited above). Our earlier results have strongly suggested that other models of spiral arms, like recurrent wave patterns with different locations of the corotation resonance during galactic life (e.g. Sellwood & Binney 2002) or with the corotation in the inner part of the Galaxy (Weinberg 1994), etc., failed to explain the bimodal radial distribution of oxygen in the galactic disc.

Some other explanations have been proposed recently for the decrease in abundances of many elements with galactocentric distance as well as for the bimodal structure of the observed gradient. These explanations are mostly centered on the radially dependent infall rate and/or star formation efficiency (see, e.g., Colavitti et al. 2009; Fu et al. 2009; Magrini et al. 2009). In various models the gradient may have both internal (inside-out disc formation) and external (dilution by metal-poor infall from the halo) origin with respect to the disc. In particular, Colavitti et al. (2009) concluded that the inside-out disc formation and the density threshold are both necessary ingredients for a model which is supposed to reproduce simultaneously all the disc constraints, including steep gradient in the inner disc and flat gradient in the outer disc. However, in studies cited above the gradient slope changes at 11–12 kpc, while observations indicate that the change occurs closer to the Galactic centre, at around 7 kpc (LKA06).

As it was noticed above, the observed radial distribution of iron is similar to oxygen. Unlike oxygen, only  $\sim 1/3$  of iron is produced by SN II. About  $2/3$  of it is synthesized during SN Ia explosions (Matteucci 2004). For a long time, precursors of these events were considered to be quite old objects with ages of the order of several (4–5) billion years. Even if they are born in spiral arms, for a long time prior to the explosion they “forget” the initial affinity to spiral arms due to both azimuthal and radial migration. So, at first sight, we should not expect strong manifestations of galactic spiral arms influence on radial distribution of iron. Hence, the similarity of bimodal radial distributions of oxygen and iron in the disc of the Galaxy represents a difficult enigma.

Recently, Manucci et al. (2006) have shown that there may exist two sub-populations of SN Ia. Events of the first type (short-lived progenitors, they were called “prompt”) have ages less than  $10^8$  years, while events of the second type (“tardy”) have long-lived progenitors, with delays between formation and explosion being measured in billions years (the theoretical basis for such kind of division see in Iben & Tutukov (1984)). The frequencies of explosions and iron outputs for both populations are approximately equal. Prompt SNe Ia precursors, being quite massive stars, retain their relation to the spiral pattern. Taking into account that SN II and short-lived SN Ia jointly produce  $\sim 2/3$  of iron, this new result opens an opportunity for solving the above problem in the framework of the theory of spiral arms influence on radial abundance distribution.

In this paper, we propose a unified mechanism for formation of bimodal radial distribution both for oxygen and iron.

## 2 OBSERVATIONAL DATA

In Fig. 1 the radial distribution of  $\langle [O/H] \rangle$  and  $\langle [Fe/H] \rangle$  vs galactocentric distance  $r$  is shown (as usual  $[X/H] =$

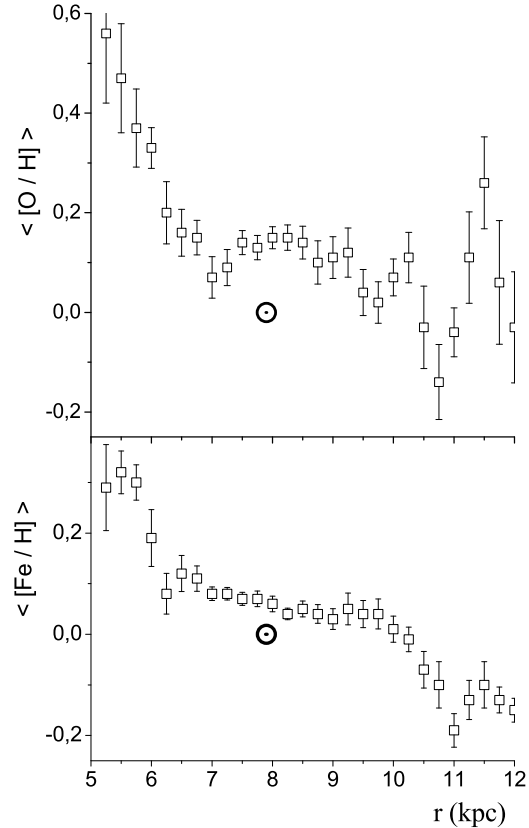


**Figure 1.** Radial distributions of oxygen (upper panel) and iron (low panel) averaged over the azimuthal angle in the galactic plane. Open squares are the observed values from Andrievsky et al. (2002) and Luck et al. (2006) averaged within bins of 0.5 kpc width. The error-like bars are the standard deviations of the corresponding mean values. The abundances of A02 and LKA06 were corrected for the new solar composition according to Asplund et al. (2006). Position of the Sun on the diagrams is shown by the usual solar mark.

$\log(N_X/N_H)_{star} - \log(N_X/N_H)_\odot$ , where  $N_{X,H}$  is the number of atoms for  $X$  element or for hydrogen, correspondingly). We divided  $r$  into bins of 0.5 kpc and averaged the corresponding data from A02 and LKA06 within each bin. The angle brackets ( $\langle \dots \rangle$ ) denote these averaged values. The error bars show the standard deviation of the averaged values within the bin. We used the solar galactocentric distance  $r_\odot = 7.9$  kpc, as in LKA06, but abundances were corrected for the new solar composition (Asplund et al. 2006). In this figure, the Sun is shown by the usual mark. The similar bimodal patterns in oxygen and iron radial distribution are clearly seen in Fig. 1.

Our aim is to explain the bimodal radial distribution of oxygen and iron in the most part of the Galaxy, i.e. the steep gradient in the inner part of the Galactic disc ( $r \leq 7$  kpc) and rather shallow distribution up to about 10 kpc with a bending at approximately 7 kpc. The peculiarities in the distributions at  $r > 10$  kpc are beyond the scope of our theory.

### 3 BASIC EQUATIONS AND MODEL

The equations of chemical evolution of ISM are close to the ones of Tinsley (1980), Chiosi (1980), Lacey & Fall (1985):

$$\dot{\mu}_g = f - \psi + \int_{m_L}^{m_U} (m - m_w) \psi(t - \tau_m) \phi(m) dm, \quad (1)$$

$$\begin{aligned} \dot{\mu}_i &= \int_{m_L}^{m_U} (m - m_w) Z_i(t - \tau_m) \psi(t - \tau_m) \phi(m) dm + \\ &E_i^{\text{Ia}} + E_i^{\text{II}} + f Z_{i,f} + \frac{1}{r} \frac{\partial}{\partial r} \left( r \mu_g D \frac{\partial Z_i}{\partial r} \right), \end{aligned} \quad (2)$$

where  $\mu_{g,i}$  are surface mass densities for interstellar gas (subscript “g”) and heavy elements (where subscript “i” is “O” for oxygen and “Fe” for iron),  $Z_i = \mu_i / \mu_g$  is the mass fraction for the corresponding elements,  $\psi$  is the star formation rate (SFR), for which we adopt (Kennicutt 1998):

$$\psi = \nu \mu_g^{1.5}, \quad (3)$$

where  $\nu$  is a normalizing coefficient. All the above quantities are functions of time  $t$  and radius  $r$ , but we do not explicitly indicate them except for the cases when there is the time shift,  $t - \tau_m$ , in the integrals.  $m$  is the stellar mass (all masses are in solar units),  $m_L$  and  $m_U$  are the minimum and maximum stellar masses,  $m_L = 0.1$ , while for  $m_U$  we use two values 50 and 70 (Tsujimoto et al. 1995). Our calculations show that the results are very close for the both above values of  $m_U$ . That is why in our figures we only show the radial distributions for  $m_U = 70$ . The life-time of a star of mass  $m$ ,  $\tau_m$  (in Gyrs), on the main sequence is given by  $\log(\tau_m) = 0.9 - 3.8 \log(m) + \log^2(m)$  (Tutukov & Krügel 1980). The initial mass function  $\phi(m)$  is Salpeter’s one with the exponent of -2.35.

In full formulation of the problem, we should take into account the divergent terms, which describe the influence of radial gas flow (“radial inflow”) within the galactic disc. Its effect was considered in various models by Lacey & Fall (1985), Portinari & Chiosi (2000), Mishurov et al. (2002). In the present paper, we will not include the radial redistribution of the interstellar gas. This problem will be separately considered in details elsewhere.

The infall rate,  $f$ , of intergalactic gas onto the galactic disc we describe as:

$$f = B(r) \exp(-\frac{t}{t_f}).$$

For the time scale  $t_f$  the following representations were used: 1)  $t_f = 3$  Gyrs (let us call this law as “rapid” disk formation model, see Portinari & Chiosi (1999)); 2)  $t_f = 7$  Gyrs (“slow” disc formation) and 3)  $t_f = c + dr$ , where  $c$  and  $d$  are some constants. The last dependence produces the so-called “inside-out” scenario for the galactic disk formation. We consider various values for  $c$  and  $d$ . i)  $c = 1.033$ ;  $d = -1.267$  (Chiappini et al. 2001). It is obvious that this representation may not be used at  $r = 1.226$  kpc since here  $f \rightarrow 0$ . To exclude this peculiarity we use the above representation for  $r > r_f = 2 - 3$  kpc. Inside  $r_f$  let us suppose  $t_f = a + br_f = \text{const}$ . Our experiments show that in the range of galactocentric distances, interesting for us, the result does not depend on the exact value of  $r_f$ . ii)  $t_f = 1 + 0.76r$  (Fu et al. 2009). At the Sun location the both expressions give  $t_f = 7$  Gyrs.

To fix  $B(r)$  as usually we adopt that the final radial total density distribution (stars + gas) at current epoch,  $t = T_D$  ( $T_D = 10$  Gyrs is the disc age) is exponential with the radial scale

$r_d = 2.5 - 4.5$  kpc (see, e.g., Naab & Ostriker (2006), Fu et al. (2009), Schönrich & Binney (2008) and others).

In all our experiments we normalize the infall rate so that the total present-day density at the solar location to be equal to  $50 M_\odot$  (Naab & Ostriker 2006). To obtain the normalizing coefficient  $\nu$  for SFR function (see Equation (3)) we suppose that at the solar galactocentric distance  $\mu_g \approx 10 M_\odot$ .

The infalling gas is assumed to have abundances  $Z_{i,f} = 0.02 Z_{i,\odot}$ .

The value for the mass of stellar remnants (white dwarfs, neutron stars and black holes) is adopted as follows: for  $m \leq 10 m_w = 0.65 m^{0.333}$ ; in the range  $10 < m < 30 m_w = 1.4$ ; if  $30 \leq m < m_U$  the remnant is a black hole with  $m_w = 10$ ; finally for  $m \geq m_U$  the stars are black holes right away from their birth and they are removed from the nucleosynthesis and returning the mass to ISM (Mashevich & Tutukov (1988), Breton (2009), Woosley et al. (2002)).

The last term in Equation (2) describes the radial diffusion of heavy elements. We need it to smooth out strong depression in abundance distribution forming when the role of spiral arms on heavy elements synthesis is taken into account (in the case of low gradient, the role of the diffusion happens to be negligible). Note as well, that the diffusion smoothes out the element distribution as admixtures but not the gaseous density as a whole (Landau & Lifshitz (1986)). The nature of the diffusion we attribute to turbulence in ISM arising due to stellar winds, supernovae explosions, galactic fountains, etc. For a phenomenological description of this process, we introduce the diffusion term into Equation (2). To estimate the diffusion coefficient  $D$  we model the turbulent ISM by a system of clouds, so a simple gas kinetic approach enables us to derive the expression for  $D$  (see Mishurov et al. 2002; Acharova et al. 2005):

$$D = \frac{H v_T}{3\pi\sqrt{2}\mu_g} \frac{m_c}{a^2},$$

where  $H = 130$  pc is the thickness of the gaseous disc,  $v_T = 6.6 \text{ km s}^{-1}$  is the one dimensional dispersion of cloud chaotic velocity,  $m_c$  and  $a$  are the mass and radius of a typical cloud,  $m_c/a^2 = 100 M_\odot \text{ pc}^{-2}$  (Elmegreen 1987).

Enrichment rates of ISM by SN Ia and SN II, correspondingly, are set by values  $E_i^{\text{Ia}}$  and  $E_i^{\text{II}}$ . The rates of oxygen and iron synthesis in SN II events are described by similar expressions  $E_i^{\text{II}} = \eta P_i^{\text{II}} R_i^{\text{II}}$ , where  $P_i^{\text{II}}$  is the mass of ejected oxygen or iron per one SN II explosion,  $R_i^{\text{II}}$  is the rate of SNe II events

$$R_i^{\text{II}}(r, t) = (1 - A) \int_{m_8}^{m_U} \psi(r, t - \tau_m) \phi(m) dm,$$

$m_8 = 8$ ,  $A = 0.0025$ . The last parameter gives the fraction of binary systems producing SNe Ia relative to the whole mass range  $m_L \leq m \leq m_U$  (Manucci et al. 2006). The factor  $\eta$  describes the influence of spiral arms (see below).

Contribution from SN Ia to the enrichment is represented as  $E_i^{\text{Ia}} = E_{i,P} + E_{i,T}$  since there are two populations of SNe Ia progenitors, namely, short-lived (“P”) and long-lived (“T”, Manucci et al. 2006; Matteucci et al. 2006). As we wrote in Introduction, being massive stars, the short-lived progenitors are concentrated near spiral arms. So, by analogy with SN II rates we write down  $E_{i,P} = \gamma \eta P_i^{\text{Ia}} R_P^{\text{Ia}}$ , where  $\gamma$  is a correction factor. For long-lived SN Ia  $E_{i,T} = \zeta P_i^{\text{Ia}} R_T^{\text{Ia}}$ . Here  $R_{P,T}^{\text{Ia}}$  are rates of SN Ia explosions for P- and T-progenitors,  $P_i^{\text{Ia}}$  is the mass of ejected  $i$ -th element per one SN Ia event, and  $\zeta$  is another normalizing coefficient.

To compute  $R_{P,T}^{\text{Ia}}$  we follow Matteucci et al. (2006) but explicitly separate the “Delay Time Distribution” function,  $DTD(\tau)$ , into two parts:  $DTD = D_P$  for  $\tau \leq \tau_S = 10^{-1.07}$  Gyrs (P-progenitors):

$$\log(D_P) = 1.4 - 50[\log(\tau) + 1.3]^2,$$

and  $DTD = D_T$  for  $\tau > \tau_S$  (T-progenitors):

$$\log(D_T) = -0.8 - 0.9[\log(\tau) + 0.3]^2.$$

So,

$$R_P^{\text{Ia}}(r, t) = Ak_\alpha \int_{\tau_S}^t \psi(r, t - \tau) D_P(\tau) d\tau,$$

$\tau_8$  is the life-time for a star of mass  $m = 8$  and

$$R_T^{\text{Ia}}(r, t) = Ak_\alpha \int_{\tau_S}^t \psi(r, t - \tau) D_T(\tau) d\tau,$$

$$k_\alpha = \int_{m_L}^{m_U} \phi(m) dm \text{ (see details in Matteucci et al. 2006).}$$

Notice that  $D_P$  has a very sharp maximum at  $\tau = \tau_P = 10^{-1.3}$  Gyrs  $\approx 50$  Myrs. This means that for  $\tau_8 \leq t < \tau_P$  the main contribution to  $R_P^{\text{Ia}}$  comes from the vicinity of  $\tau \sim t$  whereas for  $t \geq \tau_P$  the vicinity of  $\tau_P$  is most important. The corresponding integral was computed asymptotically using the Laplace method.

To incorporate the influence of spiral arms on formation of radial abundance pattern in our theory, we follow the idea of Oort (1974). For this, we take into account that SN II and short-lived SN Ia progenitors are concentrated near spiral arms. Hence, the enrichment of any volume of ISM by heavy elements only takes place when the volume is close to the nucleosynthesis sites, i. e., inside or near spiral arms. The more frequently the volume passes an arm, the higher the rate of its enrichment gets. The frequency of the volume entering a spiral arm is proportional to the difference  $|\Omega(r) - \Omega_P|$  where  $\Omega(r)$  is the angular rotation velocity of the galactic disc,  $\Omega_P$  is the rotation velocity of the wave pattern responsible for the spiral arms. So, we write  $\eta = \beta|\Omega(r) - \Omega_P|/\Theta$ , where  $\beta$  is a normalizing coefficient,  $\Theta$  is a cutoff factor. The correction factor  $\gamma$  in expression for  $E_{i,P}$  was introduced to take into account that we aim to obtain close amounts of iron produced by SN II and prompt SN Ia.

We assume that long-lived SN Ia progenitors do not concentrate in spiral arms and are uniformly distributed over the azimuth angle in the galactic disc. Therefore, unlike  $\eta$ ,  $\zeta = \text{const}$ .

Spiral arms exist between inner,  $r_i$ , and outer,  $r_o$ , Lindblad resonances, their locations being given by the condition  $\Omega(r_i) - \kappa(r_i)/n \leq \Omega_P \leq \Omega(r_o) + \kappa(r_o)/n$ . Here,  $n$  is the number of spiral arms,  $\kappa$  is the epicyclic frequency. So in the wave zone, i. e., between Lindblad resonances,  $\Theta = 1$ , and beyond them  $\Theta = 0$ . From the galactic density wave theory (Lin et al. 1969) it is known that the density wave pattern rotates as a solid body, i. e.,  $\Omega_P = \text{const}$  whereas the galactic matter rotates differentially:  $\Omega$  is a function of the galactocentric distance  $r$ . The radius  $r_c$  where both velocities coincide ( $\Omega(r_c) = \Omega_P$ ) is called the corotation radius. In the absence of diffusion from the above representation for  $\eta$  one can expect the formation of a valley (or a gap) in the abundances distribution near the corotation (see below). The diffusion smoothes out the valley so that the combine effect of it and the corotation resonance results in formation of the bimodal radial distribution of the abundances.

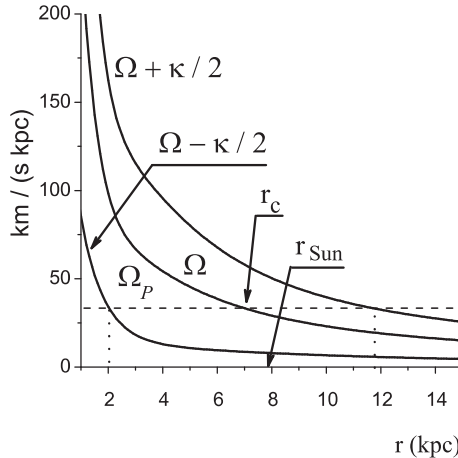


**Figure 2.** The rotation curve  $\Omega(r)$  and its combinations with epicyclic frequency  $\kappa$  approximated over the data of Clemens (1985) adjusted for  $r_\odot = 7.9$  kpc. The horizontal dashed line shows the adopted value of the angular rotation velocity,  $\Omega_P$ , for the density wave pattern which corresponds to the location of the corotation resonance at  $r_c \approx 7$  kpc. The vertical dotted lines indicate the positions of Lindblad resonances.

In our modelling we used a rotation curve based on CO data (Clemens 1985) but adjusted for  $r_\odot = 7.9$  kpc:

$$r\Omega = 260 \cdot \exp\left[-\frac{r}{150} - \left(\frac{3.6}{r}\right)^2\right] + 360 \cdot \exp\left(-\frac{r}{3.3} - \frac{0.1}{r}\right). \quad (4)$$

The rotation curve is shown in Fig. 2. Also indicated in Fig. 2 are locations of Lindblad and corotation resonances derived for  $\Omega_P = 33.3 \text{ km s}^{-1} \text{ kpc}^{-1}$  (correspondingly  $r_c \approx 7$  kpc).

Mathematically our system of equations splits into two groups. Equation (1) is an ordinary differential equation. Solving it, we find both the gaseous and stellar density radial profiles at any time  $t$ , fitting the observed stellar and gaseous densities to the ones at present time. Equations (2) are differential equations in partial derivatives. For the boundary conditions we adopt the natural ones at the galactic centre and at the galactic periphery which guarantees the finiteness of our solutions (see details in Acharova et al. 2005).

Corresponding constants for “chemical reactions” ( $\beta, \gamma, \zeta$ ) were derived in the following way. As can be seen from Matteucci (2004), Tsujimoto et al. (1995) SNe Ia produce a small part of oxygen, no more than several percents. Hence, at first step we can neglect oxygen enrichment from SNe Ia. This enables us to find independently the parameter  $\beta$  by fitting the observed radial distribution of oxygen. After that we derive other two quantities,  $\gamma$  and  $\zeta$ . To do that we impose the additional condition that short-lived (P) SN Ia, long-lived (T) SN Ia, and SN II produce equal amounts of iron ( $\sim 1/3$  each). This constraint enables to solve the problem unambiguously. The above derived values for chemical reactions constants we consider as zero order approximation for them. After that, we include the contribution to oxygen production from SN Ia and find the revised chemical constants.

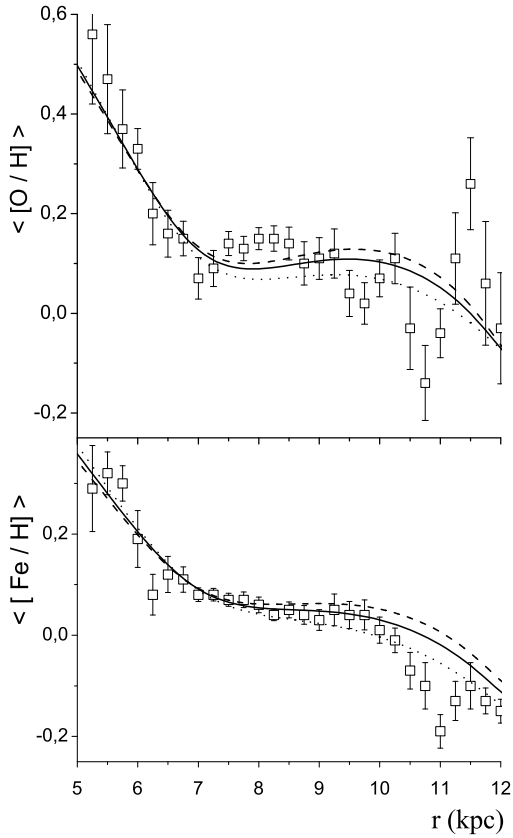


**Figure 3.** Theoretical abundance patterns derived for constant  $t_f = 3$  Gyrs (rapid disc formation model) superimposed on the observations. *Dotted lines* are for  $r_d = 2.5$  kpc. *Solid lines* – for  $r_d = 3.5$  kpc. *Dashed lines* – for  $r_d = 4.5$  kpc.

#### 4 RESULTS AND DISCUSSION

Below we show the results of our modeling for the adopted value of  $\Omega_P$  which corresponds to the location of the corotation resonance at  $r_c \approx 7$  kpc.<sup>1</sup>

In Fig. 3 and Fig. 4 are shown the computed abundance patterns for constant  $t_f$ . In the case of rapid disc formation ( $t_f = 3$  Gyrs) we demonstrate the dependence of the distributions on the radial scale  $r_d$ . It is seen that in the inner part of the disc the corresponding curves are indistinguishable. They slightly differ beyond the solar location. Overall, the coincidence of the model with the observations is good but perhaps it is the best for the radial scale  $r_d = 3.5$  kpc.

In the case of slow disc formation ( $t_f = 7$  Gyrs, Fig. 4) we failed to fit the model to the observations. The matter is, by means of one set of chemical constants we can fit the observations, say, in the inner part of the disc, but for matching with the data in the outer part we have to use another set of the constants.

The general conclusion is: in the framework of scenario of disc formation with constant  $t_f$  we can succeed in agreement with

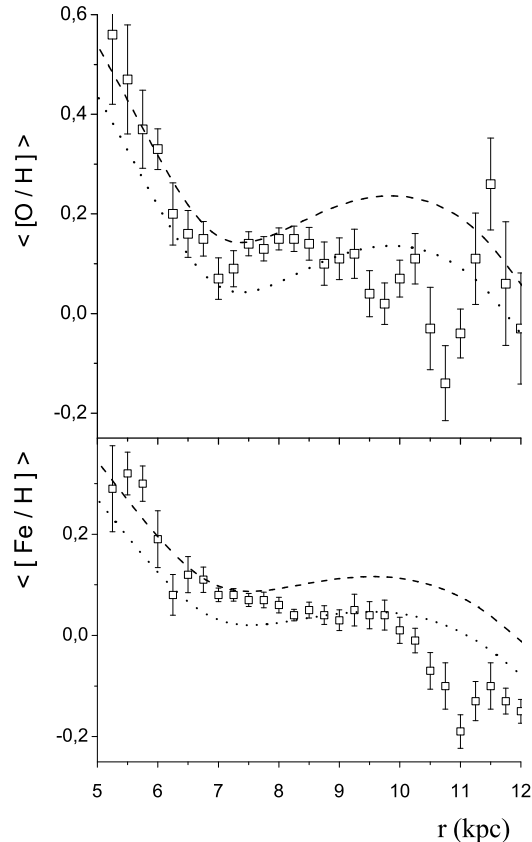


**Figure 4.** The same as in Fig. 3 but for  $t_f = 7$  Gyrs (slow disc formation model) and  $r_d = 3.5$  kpc. *Dotted lines* are for the set of the fitting parameters  $\beta = 0.030$ ,  $\gamma = 0.32$ ,  $\zeta = 0.22$ . *Dashed lines* are for the set  $\beta = 0.037$ ,  $\gamma = 0.30$ ,  $\zeta = 0.25$ . From this figure is seen that there is no way to reconcile the model with the observational data in all range of galactic radius by means of the same set of chemical constants.

the observed radial distributions both for oxygen and iron in the galactic disc with short time scale  $t_f \sim 3$  Gyrs. The fitted parameters happen to be as follows: for the upper stellar mass  $m_U = 70$   $\beta = 0.019$ ,  $\gamma = 0.44$ ,  $\zeta = 0.18$ ; for  $m_U = 50$   $\beta = 0.026$ ,  $\gamma = 0.32$ , parameter  $\zeta$  remains the same.

However, to derive the observed distributions and satisfy the condition that the above three types of sources produce approximately equal amount of iron, we had to adopt the following masses ejected per one SN. In the case  $m_U = 50$  the corresponding values are equal to the ones in Tsujimoto et al. (1995), i. e.,  $P_O^{II} = 1.80 M_\odot$ ,  $P_{Fe}^{Ia} = 0.613 M_\odot$ ,  $P_{Fe}^{II} = 0.084 M_\odot$ . For the upper value of  $m_U = 70$   $P_O^{II} = 2.47 M_\odot$ ,  $P_{Fe}^{Ia} = 0.613 M_\odot$ , like in the last cited paper but  $P_{Fe}^{II} = 0.13 M_\odot$ , (i.e. about 1.5 times greater than in Tsujimoto et al. 1995).

Our experiments show that SNIa produce about 2% of oxygen.

In Fig. 5 are shown the computed distributions for the inside-out scenario (since they are close both for the models of Chiappini et al. (2001) and Fu et al. (2009) we only show the results for Chiappini-like representation of  $t_f$ ). In our opinion the coincidence of the theory with the observations both for oxygen and iron is excellent. The chemical reactions are close to the ones of constant  $t_f$ , namely: for  $m_U = 70$   $\beta = 0.021$ ,  $\gamma = 0.46$ ,

<sup>1</sup> The above value for the corotation radius is not to be considered as a determination of  $r_c$ , it only produces a good fit to the bimodal radial distribution of oxygen and iron in a simple model that does not include all the fine effects.

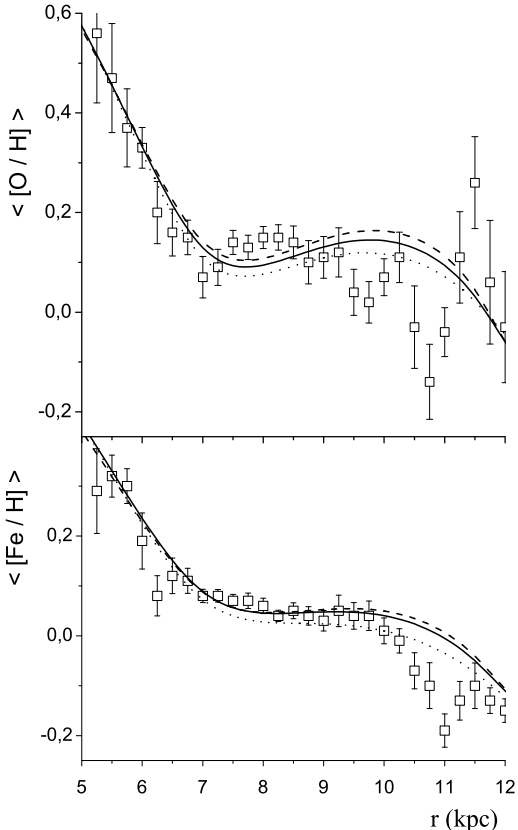


**Figure 5.** The same as in Fig. 3 but for inside-out disc formation scenario for Chiappini – like model (see Section 3) and  $r_f = 3$  kpc (in the radius range interesting for us the results slightly depend on the exact value of  $r_f$ ). Other designations are the same as in Fig. 3.

$\zeta = 0.18$ ; for  $m_U = 50$   $\beta = 0.032$ ,  $\gamma = 0.30$ , parameter  $\zeta$  again remains the same.

To feel the role of the turbulent diffusion, in Fig. 6 we show the theoretical radial distributions in the case when the diffusion coefficient is 10 times less (rather arbitrary) than the value estimated for the parameters from Section 3 (we can not put it zero since the diffusion term in Equation (2) determines the highest order of the derivative). The formation of a gap in the abundance radial distribution near the corotation in this case is obvious.

So, as it might have been expected, the main driver for the origin of the bimodal radial abundance distribution is the corotation resonance. However, in the absence of the turbulent diffusion we will have strong depression in radial distribution of heavy elements near the corotation. Hence, only combined effect of corotation and diffusion leads to a formation of the bimodal distributions both for oxygen and iron. The gradient in the inner part derived from iron is slightly shallower than the one for oxygen since  $\sim 1/3$  of iron is synthesized by long-lived SNe Ia which are not concentrated in spiral arms and are not affected by the corotation resonance.

In our theory, we aimed to construct a simplest model for explanation of bimodal radial abundance pattern formation for elements, which are synthesized by different sources with different galactic distributions. That is why we did not take into account various secondary effects like radial inflow of interstellar gas, dependence of stellar life-time on the metallicity, drift of the corotation

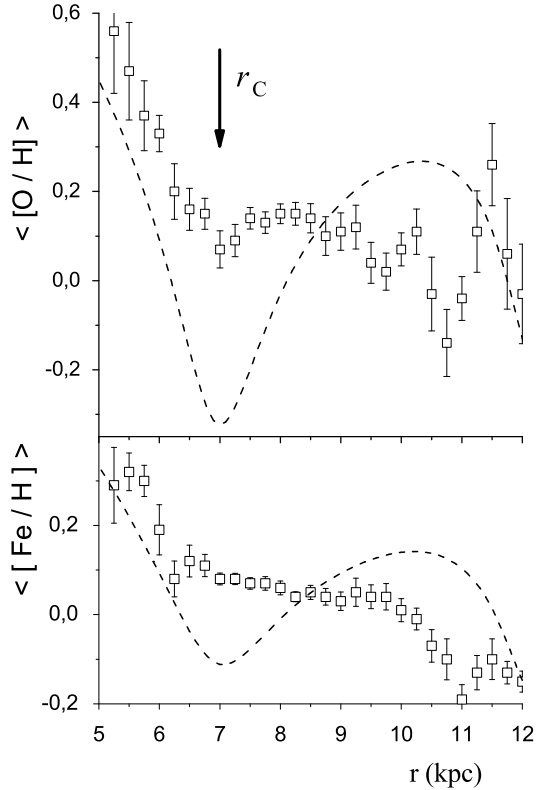


**Figure 6.** The same as in Fig. 3 but for the diffusion coefficient 10 times less and  $r_d = 3.5$  kpc. By the arrow is shown the location of the corotation resonance. The formation of the deep gap in abundances distributions near the corotation in the absence of the turbulent diffusion is obvious.

resonance, etc. Inclusion of such effects in our model will enable to develop a more precise model of formation of the bimodal distribution of heavy elements. Also, it should be noted that in the current study the proposed mechanism acts together with the radially dependent gas infall. However, it will, probably, shape the heavy element distribution in a similar manner acting in concord with other gradient formation mechanisms, like the radially dependent enriched galactic wind, as proposed by Wiebe et al. (2001). Also, as Acharova et al. (2005) have shown, the influence of spiral arms alone is able to explain the very existence of the gradient, not only its bimodal shape. In any case, the discovery of two types of SN Ia progenitors (short-lived and long-lived), made by Manucci et al. (2006), opens the opportunity to explain not only the overall gradient, but the formation of fine structure in radial distribution over the galactic disc for various heavy elements by means of a unified mechanism – the influence of the corotation resonance.

## ACKNOWLEDGMENTS

Authors are grateful to anonymous referee for very important comments.

BMS, AVT and DSW thank Russian Funds for basic research, grants no. 07-02-00454, 08-02-00371 and 4354.2008.2.

## REFERENCES

Acharova I., Lépine J., & Mishurov Yu. 2005, MNRAS, 359, 819  
 Andrievsky S., Kovtyukh V., Luck R., et al. 2002, A&A, 381, 32  
 Asplund M., Grevesse N. & Sauval, A. 2006, Comm. in Asteroseismology, 147, 76  
 Breton R. 2009, arXiv: 0907.2623v1  
 Chiappini C., Matteucci F., & Romano, D. 2001, ApJ, 554, 1044  
 Chiosi C. 1980, A & A, 83, 206  
 Clemens D. 1985, ApJ, 295, 422  
 Colavitti E., Cescutti G., Matteucci F. & Murante, G. 2009, A&A, 496, 429  
 Elmegreen B., 1987, in Hollenbach D.J., Thronson H.A., Jr., eds, Interstellar Processes, Reidel, Dordrecht, . 259  
 Fu J., Hou J. L., Yin J. & Chang, R. X. 2009, ApJ, 696, 668  
 Iben I., & Tutukov A. 1984, ApSS, 54, 335  
 Kennicutt R.C., Jr. 1998, ApJ, 498, 541  
 Lacey C.G. & Fall S.M. 1985, ApJ, 290, 154  
 Landau L. & Lifshitz E. 1986, Hydrodynamics, Nauka, Moscow  
 Lépine J., Mishurov Yu.,& Dedikov S. 2001, ApJ, 546, 234  
 Lin C., Yuan C., & Shu F. 1969, ApJ, 155, 721  
 Luck R., Kovtyukh V. & Andrievsky (LKA06), S. 2006, AJ, 132, 902  
 Magrini L., Sestito, P., Randich S. & Galli, D. 2009, A&A, 494, 95  
 Mannucci F., Della Valle M. & Panagia N. 2006, MNRAS, 370, 773  
 Massevich A. & Tutukov A. 1988, Evolution of stars: theory and observations, Nauka, Moscow  
 Matteucci F. 2004 Baryons in Dark Matter Halos in: Proceedings of Science, eds. R. Dettmar, U. Klein, P. Salucci, SISSA, Novigrad, Croatia, p.72.1  
 Matteucci F., Panagia N., Pipino, A. et al. 2006, MNRAS, 372, 265  
 Mishurov Yu., Lépine, J. & Acharova I. 2002, ApJL, 571, L113  
 Naab T. & Ostriker J. 2006, MNRAS, 366, 899  
 Oort J. 1974, IAU Symp. No. 58, *The Formation and Dynamics of Galaxies*, ed. Shakeshaft, J.R. (Dordrecht:Reidel),p. 375  
 Portinari L. & Chiosi C. 1999, A&A, 350, 827  
 Portinari L. & Chiosi C. 2000, A&A, 355, 929  
 Sellwood J. & Binney, J. 2002, MNRAS, 336, 785  
 Shaver P., McGee R., Newton L. et al. 1983, MNRAS, 204, 53  
 Schönrich R. & Binney J. 2009, MNRAS, 396, 203  
 Tinsley B.M. 1980, Fundam. Cosmic Phys., 5, 287  
 Tsujimoto T., Nomoto K., Yoshii Y. et al. 1995, MNRAS, 277, 945  
 Twarog B., Ashman K., & Anthony-Twarog B. 1997, AJ, 114, 2556  
 Tutukov A., & Krügel E. 1980, Soviet Astronomy, 24, 539  
 Weinberg M. 1994, ApJ, 420, 597  
 Wiebe D., Tutukov A. & Shustov B. 2001, Astronomy Reports, 45, 854  
 Wielen R., Fuchs B. & Dettbarn C. 1996, A&A, 314, 438  
 Woosley S., Heger A. & Weaver T. 2002, Rev Modern Phys, 74, 1015